IEEE Access
Multidisciplinary | Rapid Review | Open Access Journal

Received 6 August 2023, accepted 19 August 2023, date of publication 24 August 2023, date of current version 30 August 2023.

Digital Object Identifier 10.1109/ACCESS.2023.3308156

RESEARCH ARTICLE

Speed Tracking of SPMSM via Super-Twisting Logarithmic Fast Terminal Sliding-Mode Control

MINGYUAN HU[1], HYEONGKI AHN[2], AND KWANHO YOU[1,2]
[1]Department of Smart Fab. Technology, Sungkyunkwan University, Suwon 16419, South Korea
[2]Department of Electrical and Computer Engineering, Sungkyunkwan University, Suwon 16419, South Korea

Corresponding author: Kwanho You (khyou@skku.edu)

This work was supported in part by the National Research Foundation of Korea (NRF) Grant funded by the Korea Government (MSIP) under Grant NRF-2019R1A2C1002343, and in part by the BK21 FOUR Project.

ABSTRACT This study investigates the speed control of permanent magnet synchronous motors in the presence of external load disturbances via fast terminal sliding-mode control (FTSMC). First, to enhance the speed tracking performance, a logarithmic FTSMC method based on a novel sliding surface is proposed to improve the previously introduced FTSMC. Second, we have derived an enhanced settling time, demonstrating its superiority over that of recently introduced exponential FTSMC through the utilization of a logarithmic sliding surface. Third, the proposed logarithmic FTSMC and exponential FTSMC are compared to demonstrate that the convergence time of the logarithmic FTSMC is less than that of the exponential FTSMC. Forth, super-twisting reaching law is adopted in logarithmic FTSMC to counteract perturbations since it has an ability against various unknown disturbances, such as parameter mismatch, load torque variation, and friction force. Finally, the simulation results show that the proposed strategy can effectively improve the dynamic performance and robustness of permanent magnet synchronous motor systems.

INDEX TERMS PMSM, sliding mode control, sliding surface, super-twisting reaching law, speed tracking.

ABBREVIATION LIST

FTSMC	Fast terminal sliding-mode control
LFTSMC	Logarithmic fast terminal sliding-mode control
EFTSMC	Exponential fast terminal sliding-mode control
PMSM	Permanent magnet synchronous motor
SMC	Sliding mode control
TSMC	Terminal sliding mode control
NTSMC	Nonsingular terminal sliding mode control
LMI	Linear matrix inequality
SPMSM	Surface-mounted permanent magnet synchronous motor

I. INTRODUCTION

Permanent magnet synchronous motors (PMSMs) are considered a core component of high-performance AC motor drive systems. PMSMs are widely used in electric vehicles, urban rail vehicles, and wind power generation owing to their high power factor, torque density, low acoustic noise and torque ripple [1], [2]. However, a classical linear control strategy might not guarantee high tracking performance for a PMSM because it is a multivariable, coupled, and highly nonlinear system. The issues make PMSM extremely sensitive to parameter perturbations, system uncertainties, and unavoidable external disturbances [3].

With the rapid development of control strategies, several control methods have been developed to overcome these issues and enhance tracking performance [4], [5]. Sliding mode control (SMC) has been demonstrated to be an effective method for improving the anti-disturbance ability and robustness of PMSM systems and has been improved further [6], [7]. To improve the convergence time issue of conventional SMC, terminal SMC (TSMC) is one of the earliest SMC methods that uses a nonlinear sliding surface and has the advantage of converging to a steady state in a finite time [8], [9], [10]. Because the singular

The associate editor coordinating the review of this manuscript and approving it for publication was Nasim Ullah.

value limits the applications of TSMC, Yang et al. [11] proposed a nonsingular TSMC (NTSMC) that maintained the merits of TSMC and solved the singularity problem. Because the convergence time is not optimal, a fast TSMC (FTSMC) control strategy [12], [13] was suggested to solve the issues. A linear term was appended to the surface to improve the convergence speed, where the sliding surface was proposed with a nonlinear function to ensure finite-time convergence. Based on a conventional FTSMC, an exponential FTSMC (EFTSMC) was designed that was better than the FTSMC owing to the exponential terminal sliding mode [14].

For anti-disturbance, a design scenario is formulated to develop a consensus controller that guarantees global stability despite disturbances [15]. The study explores an event-triggered mechanism as a leaderless consensus control strategy for nonlinear multi-agent systems in the presence of disturbances. Reference [16] focuses on the design of distributed observers for wireless sensor networks, considering the presence of unknown parameters and an event-triggered mechanism. The study employs a Lyapunov analysis approach to establish sufficient conditions for achieving exponential stability and disturbance rejection of the estimation error. Additionally, the paper presents the solution to matrix inequalities for determining the appropriate observer gains.

Meanwhile, some combination strategies have been developed via SMC and disturbance observer. A composite SMC algorithm combining FTSMC with an adaptive extended state disturbance observer was proposed and constructed. The strategy was applied to the PMSM current controller to achieve fast current dynamic response and robustness, weaken system chattering, and complete decoupling of the $d-q$ axis currents [17]. In [18], a refined SMC is introduced, specifically aimed at addressing time-varying disturbances by incorporating a disturbance observer. The results demonstrate notable enhancements compared to conventional SMC. Specifically, the proposed approach yields reduced overshoot, accelerated transient response, heightened control accuracy, and increased robustness when compared to traditional counterparts. In [19], an adaptive SMC strategy that used the system state error as the sliding mode surface was presented via a new sliding mode reaching law that could enable the system state to respond faster and improve the overshoot. Considering the unknown estimation error bounds of the disturbance, an adaptive law for the control system was designed to adjust the unknown estimation, and an adaptive non-singular FTSMC system was proposed [20].

Another problem with SMC is chattering. Many studies have focused on improving or suppressing chattering. The reaching law strategy can significantly restrain chattering through a reasonable design because the chattering phenomenon is caused by the unsatisfactory approaching process of the system trajectory to the sliding surface. An adaptive terminal sliding mode reaching law was proposed [21]. To augment the anti-disturbance capabilities, we have devised a backstepping nonsingular terminal sliding-mode controller. Additionally, we have developed a finite-time disturbance observer to further strengthen the system's robustness [22]. Lu et al. [23] proposed a second-order TSMC to obtain fast convergence and reduce chattering phenomena for estimating the load disturbance. To effectively reduce the chattering phenomenon and enhance the finite convergence, a fast nonsingular sliding mode surface function based on a traditional novel TSMC was developed [24].

To overcome the aforementioned issues, an LFTSMC combined with a novel logarithmic sliding surface, targeted at the PMSM speed controller, is proposed. The main contributions of this study are as follows:

1) To improve the previously introduced FTSMC in [12] and [13], our proposed LFTSMC offers accelerated convergence of the system through the utilization of a novel sliding surface.
2) By utilizing a logarithmic sliding surface, we have derived an improved settling time, which is demonstrated to be shorter than that of EFTSMC.
3) In comparison to EFTSMC introduced in [14], our proposed LFTSMC achieves a reduced settling time by deriving an optimized convergence time. This advancement leads to superior dynamic performance of the system.
4) Super-twisting reaching law is adopted in LFTSMC to counteract perturbations.

The remainder of this paper is organized as follows. In Section II, we describe the modeling of surface-mounted PMSM (SPMSM). In Section III, we present the design of a logarithmic sliding surface and finite-time derivation and provide a finite-time comparison between the LFTSMC and EFTSMC. Section IV presents the design of a speed controller using a logarithmic fast terminal sliding surface. Moreover, a stability analysis using the Lyapunov function and super-twisting reaching law is presented. The control performance is verified through simulations in Section V. Section VI summarizes the conclusions.

II. MATHEMATICAL MODEL OF PMSM

To facilitate the control design, a mathematical model in the $d-q$ coordinate system is established using an SPMSM [25], [26]

$$\begin{cases} u_d = Ri_d + L_s\dfrac{di_d}{dt} - p_n\omega_m L_s i_q, \\ u_q = Ri_q + L_s\dfrac{di_q}{dt} + p_n\omega_m L_s i_d + p_n\omega_m\psi_f, \\ J\dfrac{d\omega_m}{dt} = \dfrac{3}{2}p_n\psi_f i_q - T_L - B\omega_m, \end{cases} \tag{1}$$

where the corresponding parameters are listed in Table 1.

For SPMSM, the rotor field orientation control method can achieve a better control effect owing to the decoupled dynamics ($i_d = 0$). (1) can be changed into the following

TABLE 1. Parameters of the dynamical model of SPMSM.

Parameter	Unit	Description
u_d, u_q	V	d and q axis stator voltages
i_d, i_q	A	d and q axis stator currents
ω_m	rad/sec	Mechanical rotor angular velocity
R	Ω	Stator resistance
L_s	H	Stator inductance
J	$\mathrm{kg \cdot m^2}$	Physical inertia
B	$\mathrm{N{\cdot}m{\cdot}s/rad}$	Viscous damping
ψ_f	Wb	Magnetic flux
p_n	-	Number of poles
T_L	$\mathrm{N \cdot m}$	Load torque

mathematical model:

$$\begin{cases} \dfrac{di_q}{dt} = \dfrac{1}{L_s}\left(-Ri_q - p_n\psi_f\omega_m + u_q\right), \\ \dfrac{d\omega_m}{dt} = \dfrac{1}{J}\left(\dfrac{3p_n\psi_f}{2}i_q - T_L - B\omega_m\right). \end{cases} \tag{2}$$

The state variables of the SPMSM system are defined as follows:

$$\begin{cases} x_1 = \omega_d - \omega_m, \\ x_2 = \dot{x}_1 = \dot{\omega}_d - \dot{\omega}_m, \end{cases} \tag{3}$$

where ω_d denotes the reference speed of the motor and is typically constant. A combination of (2) and (3) can be expressed as follows [24]:

$$\begin{cases} \dot{x}_1 = \dot{\omega}_d - \dot{\omega}_m = \dfrac{1}{J}\left(\dfrac{3p_n\psi_f}{2}i_q - T_L - B\omega_m\right), \\ \dot{x}_2 = \ddot{\omega}_d - \ddot{\omega}_m \\ \quad = \ddot{\omega}_d - \dfrac{3p_n\psi_f}{2J}\cdot\dfrac{di_q}{dt} + \dfrac{\dot{T}_L}{J} + \dfrac{B}{J}\dot{\omega}_d - \dfrac{B}{J}x_2. \end{cases} \tag{4}$$

(4) can be rewritten by considering the influence of the changes in the internal parameters of the SPMSM as follows:

$$\begin{aligned} \dot{x}_2 = &\left(-\frac{B}{J} + \Delta a\right)x_2 + \left(-\frac{3p_n\psi_f}{2J} + \Delta b\right)\cdot\frac{di_q}{dt} \\ &+ \left(\frac{\dot{T}_L}{J} + \ddot{\omega}_d + \frac{B}{J}\dot{\omega}_d + \Delta c\right), \end{aligned} \tag{5}$$

where $\Delta a, \Delta b$, and Δc represent the uncertain part of the internal parameters. To handle the unknown part the equivalent perturbation variable is defined as $p(t)$. Thus, $p(t)$ can be rewritten as follows:

$$p(t) = \Delta a x_2 + \Delta b\cdot\frac{di_q}{dt} + \left(\frac{\dot{T}_L}{J} + \ddot{\omega}_d + \frac{B}{J}\dot{\omega}_d + \Delta c\right). \tag{6}$$

Assumption 1: The lumped perturbation of the system satisfies $|p(t)| \le l_p$, where $l_p > 0$.

Remark 1: The perturbations are assumed to be slowly-varying load torque disturbances whose derivatives are bounded because the variables of the SPMSM are bounded [27]. Therefore, Assumption 1 is reasonable. Hence, (4) can be changed to the state-space form as follows:

$$\begin{bmatrix} \dot{x}_1 \\ \dot{x}_2 \end{bmatrix} = \begin{bmatrix} 0 & 1 \\ 0 & -a \end{bmatrix}\begin{bmatrix} x_1 \\ x_2 \end{bmatrix} + \begin{bmatrix} 0 \\ -b \end{bmatrix}u + \begin{bmatrix} 0 \\ 1 \end{bmatrix}p(t), \tag{7}$$

where $u = di_q/dt$, $a = B/J$, and $b = 3p_n\psi_f/2J$.

III. DESIGN OF THE LOGARITHMIC SLIDING SURFACE AND FINITE-TIME DERIVATION AND COMPARISON

A. DESIGN OF THE LOGARITHMIC SLIDING SURFACE AND FINITE-TIME DERIVATION

Considering linear and terminal sliding modes, a new logarithmic fast terminal sliding surface is designed as follows:

$$\begin{aligned} s_L = &\dot{x} + \frac{\alpha x\cdot(|x|+1)}{k_L\cdot|x|}(e^{k_L\cdot\ln(|x|+1)} - 1) \\ &+ \frac{\beta x\cdot(|x|+1)}{k_L\cdot|x|}(1 - e^{-k_L\cdot\ln(|x|+1)})^{\frac{q}{p}}e^{k_L\cdot\ln(|x|+1)}. \end{aligned} \tag{8}$$

Here, $x \in \mathbb{R}$ is the state variable, α, β, and k_L are positive design parameters, and p, q are positive odd numbers.

Theorem 1: The time required to converge from any initial state $x(0) \neq 0$ to equilibrium state $x = 0$ is as follows:

$$t_L = \frac{p}{\alpha(p-q)}\ln\left(\frac{\alpha(1 - e^{-k_L\cdot\ln(|x(0)|+1)})^{\frac{p-q}{p}}}{\beta} + 1\right). \tag{9}$$

Proof: Because $s_L = \dot{s}_L = 0$, (10) can be obtained using (9) as follows:

$$\begin{aligned} &(1 - e^{-k_L\cdot\ln(|x|+1)})^{-\frac{q}{p}}(e^{-k_L\cdot\ln(|x|+1)})\frac{k_L\cdot x}{x\cdot(|x|+1)}\frac{dx}{dt} \\ &\quad + \alpha(1 - e^{-k_L\cdot\ln(|x|+1)})^{\frac{p-q}{p}} = -\beta. \end{aligned} \tag{10}$$

Let $y = \left(1 - e^{-k_L\cdot\ln(x|x+1)}\right)^{1-q/p}$, then,

$$\begin{aligned} \frac{dy}{dt} = &\frac{p-q}{p}(1 - e^{-k_L\cdot\ln(|x|+1)})^{-\frac{q}{p}} \\ &\cdot(e^{-k_L\cdot\ln(|x|+1)})\frac{k_L\cdot x}{|x|\cdot(|x|+1)}\frac{dx}{dt}. \end{aligned} \tag{11}$$

Therefore, (10) can be rewritten as:

$$\frac{dy}{dt} + \frac{p-q}{p}\alpha y = -\frac{p-q}{p}\beta. \tag{12}$$

Then solution of (12) is:

$$y = e^{-\int_0^t\frac{p-q}{p}\alpha d\tau_3}\left(\int_0^t -\frac{p-q}{p}\beta e^{\int_0^t\frac{p-q}{p}\alpha d\tau_1}d\tau_2 + C\right). \tag{13}$$

When $t = 0$ and $y(0) = C$, (14) can be obtained from (13) as follows:

$$y = -\frac{\beta}{\alpha} + \frac{\beta}{\alpha}e^{\frac{p-q}{p}\alpha t_L} + y(0)e^{-\frac{p-q}{p}\alpha t_L}. \tag{14}$$

When $x = 0$ and $y = 0$ at $t = t_L$, (15) can be obtained to simplify (14) as follows:

$$\frac{\beta}{\alpha}e^{\frac{p-q}{p}\alpha t_L} + y(0)e^{\frac{p-q}{p}\alpha t_L} = \frac{\beta}{\alpha}. \tag{15}$$

This implies

$$\left(\frac{\beta+\alpha y(0)}{\beta}\right)=e^{\frac{p-q}{p}\alpha t_L}. \tag{16}$$

Here, $y(0)=(1-e^{-k_L\cdot\ln(|x(0)|+1)})^{(p-q)/p}$. Therefore, in the sliding mode, the time to converge from any initial state $x(0)\neq 0$ to equilibrium state $x=0$ is as in (9). By setting the parameters of α,β,p,q, and k_L, the system can reach an equilibrium state within a limited time t_L. Therefore, the proof of Theorem 1 is completed. ■

B. FINITE-TIME COMPARISON: LFTSMC VS. EFTSMC

The convergence time equation of EFTSMC [14] is as follows:

$$t_E=\frac{p}{\alpha(p-q)}\ln\frac{\alpha\left(1-e^{-k_E|x(0)}\right)^{\frac{p-q}{p}}+\beta}{\beta}. \tag{17}$$

Moreover, the sliding surface of EFTSMC is indicated as [14]:

$$\begin{aligned}s_E=\dot{x}&+\frac{\alpha}{k_E}\left(e^{k_E|x|}-1\right)\mathrm{sgn}(x)\\&+\frac{\beta}{k_E}\left(1-e^{-k_E|x|}\right)^{\frac{q}{p}}e^{k_E|x|}\mathrm{sgn}(x).\end{aligned} \tag{18}$$

Theorem 2: The time (t_L) of LFTSMC is less than the time (t_E) of EFTSMC owing to $t_L-t_E<0$.

Proof: The process of time comparison between EFTSMC and LFTSMC is shown as follows:

$$\begin{aligned}t_L-t_E&=\frac{p}{\alpha(p-q)}\ln\frac{\alpha(1-e^{-k_L\cdot\ln(|x(0)|+1)})^{\frac{p-q}{p}}+\beta}{\beta}\\&\quad-\frac{p}{\alpha(p-q)}\ln\frac{\alpha(1-e^{-k_E|x(0)|})^{\frac{p-q}{p}}+\beta}{\beta}\\&=\frac{p}{\alpha(p-q)}(\ln H),\end{aligned} \tag{19}$$

where

$$H=\frac{\alpha(1-e^{-k_L\cdot\ln(|x(0)|+1)})^{\frac{p-q}{p}}+\beta}{\alpha(1-e^{-k_E|x(0)|})^{\frac{p-q}{p}}+\beta}.$$

According to the property of the logarithmic function, if H in (19) is between 0 and 1, then t_L-t_E is less than 0. Therefore, (20) can be obtained as follows:

$$\alpha(1-e^{-k_L\cdot\ln(|x(0)|+1)})^{\frac{p-q}{p}}+\beta<\alpha(1-e^{-k_E|x(0)|})^{\frac{p-q}{p}}+\beta. \tag{20}$$

Proceeding further to simplify (20), (21) is expressed as:

$$\left(\frac{1-e^{-k_L\cdot\ln(|x(0)|+1)}}{1-e^{-k_E|x(0)|}}\right)^{\frac{p-q}{p}}<1. \tag{21}$$

If (21) is to be established, it must satisfy $e^{-k_L\cdot\ln(|x(0)|+1)}>e^{-k_E|x(0)|}$. Hence, (22) can be obtained as follows:

$$\ln e^{-k_L\cdot\ln(|x(0)|+1)}>\ln e^{-k_E|x(0)|}. \tag{22}$$

Then, (22) can be rewritten as:

$$k_E|x(0)|-k_L\cdot\ln(|x(0)|+1)>0. \tag{23}$$

A new function $T(t)$ is defined via (23) as:

$$T(t)=k_E|x(t)|-k_L\cdot\ln(|x(t)|+1). \tag{24}$$

If $T(t)>0$, it can be proved that (23) is greater than zero. Taking the derivative of (24), (25) can be written as:

$$\dot{T}(t)=k_E\frac{x(t)}{|x(t)|}-\frac{k_L\cdot x(t)}{|x(t)|\cdot(|x(t)|+1)}. \tag{25}$$

When $k_L\leq k_E$, $\dot{T}(t)$ is always greater than or equal to zero. As $|x(t)|$ is greater than or equal to zero still holds, $T(t)$ is greater than or equal to zero is also true. Hence, $t_L-t_E<0$ can be proved. Therefore, Theorem 2 is proved. ■

IV. DESIGN OF THE SPEED CONTROLLER AND STABILITY ANALYSIS

A. DESIGN OF THE SPEED CONTROLLER VIA LOGARITHMIC FAST TERMINAL SLIDING SURFACE

Speed controller $\left(i_q^*\right)$ is derived based on the proposed logarithmic fast terminal sliding surface. Moreover, super-twisting was adopted to the controller $\left(i_q^*\right)$ to guarantee stability and suppress disturbances.

Theorem 3: The speed control of SPMSM using (4), (7), and (8) is given as:

$$\begin{aligned}i_q^*&=\frac{1}{b}\int_0^t\left(\frac{d}{dt}\left(\frac{\alpha x_1\cdot(|x_1|+1)}{k_L\cdot|x_1|}(e^{k_L\cdot\ln(|x_1|+1)}-1)\right)\right.\\&\quad+\frac{d}{dt}\left(\frac{\beta x_1\cdot(|x_1|+1)}{k_L\cdot|x_1|}(1-e^{-k_L\cdot\ln(|x_1|+1)})^{\frac{q}{p}}e^{k_L\cdot\ln(|x_1|+1)}\right)\\&\quad\left.-ax_2-k_1|s_L|^{\frac{1}{2}}\mathrm{sgn}(s)-k_2\int_0^t\mathrm{sgn}(s)d\tau_2\right)d\tau_1.\end{aligned} \tag{26}$$

Proof: As $s_L=\dot{s}_L=0$, (8) can be written via (4) as (27).

$$\begin{aligned}\dot{s}_L&=\dot{x}_2+\frac{d}{dt}\left(\frac{\alpha x_1\cdot(|x_1|+1)}{k_L\cdot|x_1|}(e^{k_L\cdot\ln(|x_1|+1)}-1)\right)\\&\quad+\frac{d}{dt}\left(\frac{\beta x_1\cdot(|x_1|+1)}{k_L\cdot|x_1|}(1-e^{-k_L\cdot\ln(|x_1|+1)})^{\frac{q}{p}}e^{k_L\cdot\ln(|x_1|+1)}\right).\end{aligned} \tag{27}$$

Combining (27) with (7), (28) is expressed as follows:

$$\begin{aligned}\dot{s}_L&=-ax_2-bu\\&\quad+\frac{d}{dt}\left(\frac{\alpha x_1\cdot(|x_1|+1)}{k_L\cdot|x_1|}(e^{k_L\cdot\ln(|x_1|+1)}-1)\right)\\&\quad+\frac{d}{dt}\left(\frac{\beta x_1\cdot(|x_1|+1)}{k_l\cdot|x_1|}(1-e^{-k_L\cdot\ln(|x_1|+1)})^{\frac{q}{p}}e^{k_L\cdot\ln(|x_1|+1)}\right).\end{aligned} \tag{28}$$

To obtain better performance, the super-twisting reaching law is chosen as [28]:

$$\dot{s}_L=-k_1|s_L|^{\frac{1}{2}}\mathrm{sgn}(s_L)-k_2\int_0^t\mathrm{sgn}(s_L)d\tau \tag{29}$$

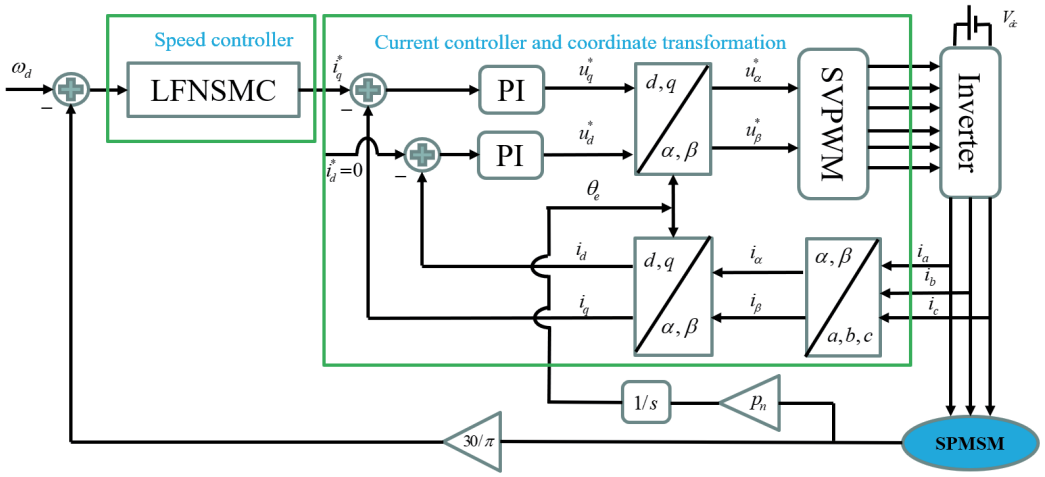

FIGURE 1. SPMSM control scheme.

where k_1 and k_2 are the positive constants. Combining (28) and (29), (26) can be derived. Hence, Theorem 3 is proved. ■

B. STABILITY ANALYSIS USING THE LYAPUNOV FUNCTION AND SUPER-TWISTING REACHING LAW

The super-twisting sliding mode algorithm is an outstanding and well-known robust control algorithm that handles a system using a relative degree equal to one. The entire procedure for stability analysis follows [29]. The closed-loop sliding dynamics, including disturbance, is designed based on the super-twisting algorithm and (28), as follows:

$$\dot{s}_L = -k_1 |s_L|^{\frac{1}{2}} \operatorname{sgn}(s_L) - k_2 \int_0^t \operatorname{sgn}(s_L)\, \mathrm{d}\tau + p(t), \quad (30)$$

where $\mathrm{x} \in \mathbb{R}^n$ denotes the state vector, $s_L = s_L(\mathrm{x}, t) \in \mathbb{R}$ represents the sliding surface, $p(t) \in \mathbb{R}$ implies an unknown perturbation in Assumption 1, and gain pair (k_1, k_2) is to be constructed such that the sliding mode can occur within a finite time. Generally, the representation of (30) is transformed into the following state-space forms:

$$\begin{aligned} \dot{z}_1 &= -k_1 |z_1|^{\frac{1}{2}} \operatorname{sgn}(z_1) + z_2, \\ \dot{z}_2 &= -k_2 \operatorname{sgn}(z_1) + \delta, \end{aligned} \quad (31)$$

that implies $z_1 = s(x, t)$ and $z_2 = -k_2 \int_0^t \operatorname{sgn}(s)\mathrm{d}\tau + \mathrm{d}(t)$, respectively, where $\delta(t) = \dot{p}(t)$ and $|\delta(t)| = |\dot{p}(t)| \le l_p$. The following variable transformations are considered because (31) is nonlinear [30].

$$\begin{aligned} \zeta_1 &= |z_1|^{\frac{1}{2}} \operatorname{sgn}(z_1), \\ \zeta_2 &= z_2. \end{aligned} \quad (32)$$

By taking the derivatives of (32) with respect to time (t), the corresponding result is expressed as follows:

$$\begin{aligned} \dot{\zeta}_1 &= \frac{1}{|z_1|^{\frac{1}{2}}} \left(-\frac{k_1}{2} |z_1|^{\frac{1}{2}} \operatorname{sgn}(z_1) + \frac{1}{2} z_2 \right) \\ &= \frac{1}{|\zeta_1|} \left(-\frac{k_1}{2} \zeta_1 + \frac{1}{2} \zeta_2 \right), \\ \dot{\zeta}_2 &= -k_2 \operatorname{sgn}(z_1) + \delta \\ &= \frac{1}{|z_1|^{\frac{1}{2}}} \left(-k_2 |z_1|^{\frac{1}{2}} \operatorname{sgn}(z_1) + |z_1|^{\frac{1}{2}} \delta \right) \\ &= \frac{1}{|\zeta_1|} \left(-k_2 \zeta_1 + |\zeta_1| \delta \right), \end{aligned} \quad (33)$$

that can be reformulated in a matrix form as follows:

$$\dot{\zeta} = \frac{1}{|\zeta_1|} (\mathbf{A}\zeta + \mathbf{B}\delta), \quad (34)$$

where

$$\begin{aligned} A &= \begin{bmatrix} -0.5k_1 & 0.5 \\ -k_2 & 0 \end{bmatrix}, \quad B = \begin{bmatrix} 0 \\ 1 \end{bmatrix}, \\ \zeta &= [\zeta_1, \zeta_2]^T, \quad |\zeta_1| = |z_1|^{\frac{1}{2}}. \end{aligned}$$

Assumption 2: Disturbance transformation $\tilde{\delta}(t, \zeta_1) = \delta(t) \cdot |\zeta_1|$ satisfies $\left|\tilde{\delta}(t, \zeta_1)\right| \le l_p |\zeta_1|$.

Remark 2: Assumption 2 is reasonable via Assumption 1 and Remark 1. In this section, the stability problem is to be proved for (34). The results show that the stability problem can be reformulated as a feasibility problem based on linear matrix inequality (LMI). By considering the dynamics model (7) of the SPMSM, the speed controller is designed as shown in (26). With the designed controllers, the speed controller guarantees asymptotic stability.

Theorem 4: Suppose that there exist symmetric and positive definite matrices $\mathbf{P} = \mathbf{P}^\top > 0$ *and* $\mathbf{Q}_c = \mathbf{Q}_c^T > 0$ *such that the following LMI [29], [31], [32], [33]*

$$\begin{bmatrix} \mathbf{PA} + \mathbf{A}^T\mathbf{P} + \mathbf{Q}_c + \mathbf{C}^T\mathbf{C} & \mathbf{PB} \\ \mathbf{B}^T\mathbf{P} & -\gamma^2 \end{bmatrix} < 0 \quad (35)$$

is feasible, where $\gamma = 1/\rho$ *and* $\mathbf{C} = \begin{bmatrix} 1 & 0 \end{bmatrix}$. *The quadratic form of the Lyapunov candidate function is used to verify the system stability. Thus, the state trajectory of the closed-loop system is driven globally to a sliding surface in finite time. The Lyapunov function is expressed as follows*:

$$V = \zeta^T \mathbf{P} \zeta, \quad (36)$$

which is a strict Lyapunov function for (34) and the initial state can reach the equilibrium point within a finite time.

Proof: Applying the Rayleigh inequality, V is bounded by

$$\lambda_{\min}(\mathbf{P})\|\zeta\|^2 \leq V \leq \lambda_{\max}(\mathbf{P})\|\zeta\|^2, \tag{37}$$

where $\lambda_{\min}$ and $\lambda_{\max}$ represent the minimum and maximum eigenvalues, respectively. $\|\zeta\|^2 = |z_1| + z_2^2$ is the Euclidean norm of ζ. Taking the time derivative of (36), (38) can be obtained as follows:

$$\dot{V} = \frac{1}{|\zeta|}\left[\zeta^T\left(\mathbf{PA} + \mathbf{A}^T\mathbf{P}\right)\zeta + \zeta^T\mathbf{PB}\tilde{\delta} + \tilde{\delta}\mathbf{B}^T\mathbf{P}\zeta\right]. \tag{38}$$

The inequality about disturbance is satisfied via Assumptions 1 and 2 as follows:

$$\left|\tilde{\delta}\left(t, \zeta_1\right)\right|^2 \leq l_p^2\left|\zeta_1\right|^2 \leq l_p^2\left(\zeta_1^2 + \zeta_2^2\right), \tag{39}$$

which guarantees

$$\zeta^r\zeta - \frac{1}{l_p^2}\tilde{\delta}\left(t, \zeta_1\right)^2 > 0. \tag{40}$$

Hence, (38) can be rewritten as follows:

$$\begin{aligned}
\dot{V} &\leq \frac{1}{|\zeta_1|}\left[\zeta^T\left(PA + A^TP\right)\zeta + \zeta^TPB\tilde{\delta}\right. \\
&\quad \left. + \tilde{\delta}B^TP\zeta + \zeta^T\zeta - \frac{1}{l_p^2}\tilde{\delta}^2\right] \\
&= \frac{1}{|\zeta_1|}\left[\zeta^T\left(PA + A^TP + C^TC + Q_c - Q_c\right)\zeta\right. \\
&\quad \left. + \zeta^TPB\tilde{\delta} + \tilde{\delta}B^TP\zeta - \frac{1}{l_p^2}\tilde{\delta}^2\right] \\
&= -\frac{1}{|\zeta_1|}\zeta^TQ_c\zeta + \frac{1}{|\zeta_1|}\begin{bmatrix}\zeta \\ \tilde{\delta}\end{bmatrix}^T \\
&\quad \cdot \begin{bmatrix}PA + A^TP + Q_c + C^TC & PB \\ B^TP & -\gamma^2\end{bmatrix}\begin{bmatrix}\zeta \\ \tilde{\delta}\end{bmatrix}.
\end{aligned} \tag{41}$$

(41) is less than zero via (35) and $\mathbf{Q}_c > 0$. Thus, Theorem 4 is proved. ∎

Theorem 5: A feasible solution, $\mathbf{P}, \mathbf{Q}_c$ exists such that the LMI given by (35) can be established if and only if parameters k_1 and k_2 in $\mathbf{A}$ satisfy the following condition [29], [31], [32], [33]:

$$k_2 > \rho, k_1^2 > 4k_2. \tag{42}$$

Alternatively,

$$k_1^2\left(\frac{1}{2}k_2 - \frac{1}{16}k_1^2\right) < \rho^2, \quad 4\,k_2 > k_1^2. \tag{43}$$

Moreover, additional constraints $k_2 \neq 0$ for (42) and $k_1 \neq 0, k_1^2 \neq 8\,k_2$ for (43) must be satisfied.

Proof: If the LMI of (34) is feasible, then the $\mathcal{L}_2$ gain of (44) must be less than or equal to γ as follows:

$$M(s) = \frac{1/2}{s^2 + (1/2)k_1 s + (1/2)k_2}; \tag{44}$$

that is,

$$\max_{\omega}|M(j\omega)| < \gamma = \frac{1}{\rho} \Rightarrow \max_{\omega}|M(j\omega)|^2 < \frac{1}{\rho^2}. \tag{45}$$

This statement is a well-known bounded real condition [34], [35]. To determine appropriate parameters (k_1, k_2) in (44), such that the condition of (45) is satisfied, $|M(j\omega)|^2$ and its derivative are obtained as follows:

$$|M(j\omega)|^2 = \frac{1}{\left(k_2 - 2\omega^2\right)^2 + (k_1\omega)^2}, \tag{46}$$

$$\frac{\mathrm{d}}{\mathrm{d}\omega}|M(j\omega)|^2 = -\frac{16\omega\left(\omega^2 + (1/8)k_1^2 - (1/2)k_2\right)}{\left[\left(k_2 - 2\omega^2\right)^2 + (k_1\omega)^2\right]^2}. \tag{47}$$

The extreme point can be derived by setting (47) equal to zero. Therefore, $\max_{\omega} M|(j\omega)|$ can be deduced to be reached by checking for second-order sufficient condition $\mathrm{d}^2|M(j\omega)|^2/\mathrm{d}\omega^2$ when the following conditions are satisfied.

$$\omega = \begin{cases} 0, & \text{if } 4\,k_2 - k_1^2 < 0, \\ \left(\dfrac{4k_2 - k_1^2}{8}\right)^{1/2}, & \text{if } 4\,k_2 - k_1^2 > 0. \end{cases} \tag{48}$$

Substituting (48) in (46) yields the corresponding maximum value of (49) as:

$$\begin{aligned}
&\max_{\omega}|M(j\omega)|^2 \\
&= \begin{cases} \dfrac{1}{k_2^2}, & \text{if } 4\,k_2 - k_1^2 < 0, \\ \dfrac{1}{k_1^2\left((1/2)k_2 - (1/16)k_1^2\right)}, & \text{if } 4\,k_2 - k_1^2 > 0. \end{cases}
\end{aligned} \tag{49}$$

Hence, the LMI (35) is feasible after combining (45) and (49), if the following conditions are satisfied as in (42).

$$k_1^2\left(\frac{1}{2}k_2 - \frac{1}{16}k_1^2\right) > \rho^2, \quad 4\,k_2 > k_1^2. \tag{50}$$

Moreover, constraints $k_2 \neq 0$ for (42) and $k_1 \neq 0, k_1^2 \neq 8\,k_2$ for (50) are considered to avoid the singularity of (49). Hence, Theorem 5 is proved. ∎

Remark 3: System (44) is the corresponding linear system of the LMI expressed by (35), instead of the transfer function of (34) [35].

V. SIMULATION

To demonstrate that the LFTSMC has a better control performance than the EFTSMC, $i_d = 0$ was employed, as shown in Fig. 1. The parameters and their SPMSM values are listed in Table 2. The controller parameters are listed in Table 3. To demonstrate the good anti-perturbation performance of the designed controller, the $p(t)$ is set to a random perturbation $(-0.2 + 0.4 \cdot rand(t))$. In this paper, we adjusted the control parameters in the simulation after many trial-and-errors. Considering the steady-state error, the

TABLE 2. Parameter values of the SPMSM.

Parameter	Value	Unit
Resistance R	0.1763	Ω
Inductance L_s	-1.95×10^{-4}	mH
Magnetic flux ψ_f	0.0109	Wb
Physical inertia J	5.8×10^{-4}	$\mathrm{kg \cdot m^2}$
Viscous damping B	1.59×10^{-4}	$\mathrm{N \cdot m \cdot s/rad}$
Pole pairs n_p	5	-

TABLE 3. Parameter values of the controller.

Parameter	Value
α	5
β	3
p	3
q	1
k_1	51
k_2	70
$k_L = k_E$	0.01

convergence speed and the stability of speed response, the final control parameters were selected.

To present the comparison and analysis results, three different cases were considered to illustrate the performance of the LFTSMC. Case I involved a sudden acceleration simulation, where the desired speed was increased by 1100 r/min at 5 s. As shown in Fig. 2(a), the LFTSMC could track the desired speed of 1000 r/min in 0.01 s whereas EFTSMC took 4.5 s, resulting in 4.49 s reduction in settling time. Both controllers responded quickly to sudden speed changes; however, later, the EFTSMC could not track the desired speed well, whereas the LFTSMC could consistently maintain the desired speed. Fig. 2(b) shows the corresponding changes in current $i_q^*(t)$ and control input. As shown in Fig. 2(b), the LFTSMC current changed smoothly and without considerable jitter compared with the EFTSMC.

Remark 4: To ensure the reliability of the simulation, the same control parameters were used for the LFTSMC and EFTSMC. Because $k_L \leq k_E$ was set as in Theorem 2, $k_L = k_E$ can be considered in Table 3. Moreover, k_E was set to be less than 0.5 [14]. We followed Theorem 2 from [14] to set the parameters in this study.

Case II involved a sudden loading simulation, as shown in Fig. 3, where an abrupt load was applied to the SPMSM at 5 s. An extra constant load torque of 0.8 $N \cdot m$ was applied for a duration of 1 s, specifically from 5 s to 6 s in Fig. 3(a). As shown in Fig. 3(a), LFTSMC could track the desired speed of 1000 r/min in 0.01 s before a sudden loading was activated whereas the EFTSMC took 4.5 s, which leads to a decrease in settling time by 4.49 s. A gap existed between the speed of the EFTSMC and the desired speed after sudden loading, and the LFTSMC could track the desired speed well despite the slight jitter. Fig. 3(b) shows the corresponding current variations for the control input. The EFTSMC exhibited sharp jitter and spikes after loading, whereas the LFTSMC exhibited a smooth variation in current without considerable jitter.

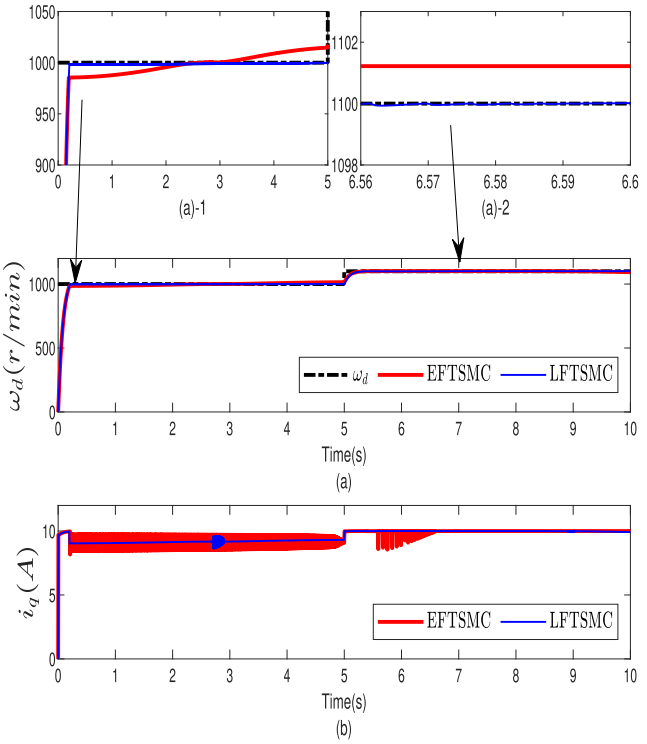

FIGURE 2. Comparison between EFTSMC and LFTSMC under sudden speed increase: (a) speed tracking, (b) control action.

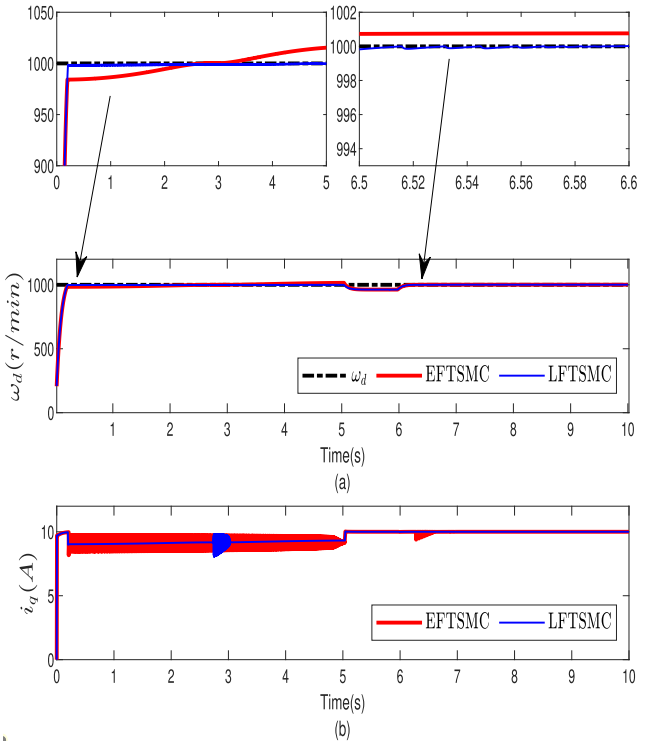

FIGURE 3. Comparison between EFTSMC and LFTSMC under sudden load: (a) speed regulation, (b) control action.

Case III involved a speed tracking simulation, as shown in Fig. 4, where the desired speed suddenly changed at 2 s, 3 s, 5 s, 7 s, and 8 s. As shown in Fig. 4(a), when the

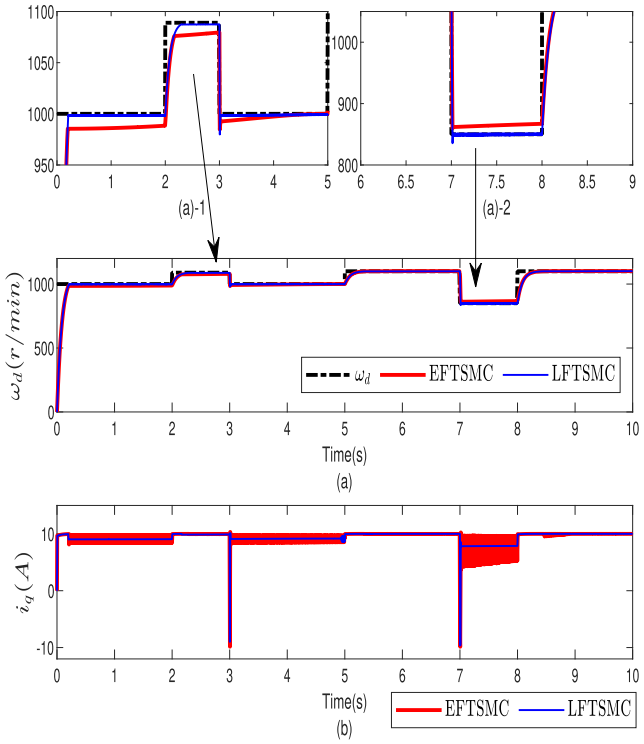

FIGURE 4. Comparison between EFTSMC and LFTSMC: (a) speed tracking, (b) control action.

desired speed suddenly changed, the LFTSMC could track the desired speed rapidly and accordingly. As shown in Fig. 4(a)-1, the LFTSMC showed good tracking performance compared with the EFTSMC when the desired speed was increased from 1000 r/min to 1090 r/min and decreased from 1090 r/min to 1000 r/min at 2 s and 3 s, respectively. Furthermore, the changes in speed at 7 s and 8 s and the corresponding behavior of the control are clearly shown in the magnified view in Fig. 4(a)-2. Fig. 4(b) shows the current variation corresponding to that in Fig. 4(a). The EFTSMC jitter was noticeable and more intense after sudden speed changes. However, the LFTSMC current continued to change smoothly.

Although random perturbations were introduced in Case I, II, and III, the simulation results remained unaffected due to the robust disturbance rejection capability of the super-twisting reaching law. This can be observed in Figs. 2, 3, and 4, where the impact of perturbations on the simulation results is negligible.

VI. CONCLUSION

In this study, an SPMSM control strategy based on a modified FTSMC theory was proposed, in which a speed controller was designed using an improved logarithmic sliding surface. Furthermore, the settling time of the improved logarithmic sliding surface was derived. The proposed sliding surface showed a faster convergence speed than the EFTSMC, and a corresponding time comparison was provided. To obtain better performance and restrain chattering, the super-twisting reaching law was chosen instead of the saturation function. Moreover, the stability of the speed dynamics was guaranteed via the algebraic Lyapunov function. Finally, the simulation results verified that the proposed strategy could effectively improve the response speed of the system in different cases. In future work, the ongoing experimental results with PMSM hardware will be complemented by utilizing the simulation processed in this study. The proposed controller demonstrates promising potential for application in PMSM, exhibiting enhanced performance.

REFERENCES

[1] W. Wang, Y. Feng, Y. Shi, M. Cheng, W. Hua, and Z. Wang, "Direct thrust force control of primary permanent-magnet linear motors with single DC-link current sensor for subway applications," *IEEE Trans. Power Electron.*, vol. 35, no. 2, pp. 1365–1376, Feb. 2020.

[2] L. Qu, W. Qiao, and L. Qu, "Active-disturbance-rejection-based sliding-mode current control for permanent-magnet synchronous motors," *IEEE Trans. Power Electron.*, vol. 36, no. 1, pp. 751–760, Jan. 2021.

[3] X. Guo, S. Huang, Y. Peng, K. Lu, S. Huang, D. Luo, and X. Wu, "An improved integral sliding mode control for PMSM drives based on new variable rate reaching law with adaptive reduced-order PI observer," *IEEE Trans. Transport. Electrific.*, early access, Feb. 3, 2023, doi: 10.1109/TTE.2023.3242452.

[4] C. Chatri, M. Labbadi, M. Ouassaid, K. Elyaalaoui, and Y. El Houm, "Design and implementation of finite-time control for speed tracking of permanent magnet synchronous motors," *IEEE Control Syst. Lett.*, vol. 7, pp. 721–726, 2023.

[5] Q. Hou and S. Ding, "Finite-time extended state observer-based super-twisting sliding mode controller for PMSM drives with inertia identification," *IEEE Trans. Transport. Electrific.*, vol. 8, no. 2, pp. 1918–1929, Jun. 2022.

[6] Z. Yin, L. Gong, C. Du, J. Liu, and Y. Zhong, "Integrated position and speed loops under sliding-mode control optimized by differential evolution algorithm for PMSM drives," *IEEE Trans. Power Electron.*, vol. 34, no. 9, pp. 8994–9005, Sep. 2019.

[7] F. M. Zaihidee, S. Mekhilef, and M. Mubin, "Application of fractional order sliding mode control for speed control of permanent magnet synchronous motor," *IEEE Access*, vol. 7, pp. 101765–101774, 2019.

[8] S. Li, M. Zhou, and X. Yu, "Design and implementation of terminal sliding mode control method for PMSM speed regulation system," *IEEE Trans. Ind. Informat.*, vol. 9, no. 4, pp. 1879–1891, Nov. 2013.

[9] W. Xu, A. K. Junejo, Y. Liu, and Md. R. Islam, "Improved continuous fast terminal sliding mode control with extended state observer for speed regulation of PMSM drive system," *IEEE Trans. Veh. Technol.*, vol. 68, no. 11, pp. 10465–10476, Nov. 2019.

[10] C. Mu and H. He, "Dynamic behavior of terminal sliding mode control," *IEEE Trans. Ind. Electron.*, vol. 65, no. 4, pp. 3480–3490, Apr. 2018.

[11] Z. Yang, D. Zhang, X. Sun, W. Sun, and L. Chen, "Nonsingular fast terminal sliding mode control for a bearingless induction motor," *IEEE Access*, vol. 5, pp. 16656–16664, 2017.

[12] B. Zhang, B. Deng, X. Gao, W. Shang, and S. Cong, "Design and implementation of fast terminal sliding mode control with synchronization error for cable-driven parallel robots," *Mechanism Mach. Theory*, vol. 182, Apr. 2023, Art. no. 105228.

[13] X. Yu and M. Zhihong, "Fast terminal sliding-mode control design for nonlinear dynamical systems," *IEEE Trans. Circuits Syst. I, Fundam. Theory Appl.*, vol. 49, no. 2, pp. 261–264, Feb. 2002.

[14] T. Zhu, Y. Xiao, H. Zhang, and Y. Pan, "Trajectory tracking control of USV based on exponential global fast terminal sliding mode control," Res. Square, Tech. Rep., Jan. 2022, pp. 1–12.

[15] I. Ahmed, M. Rehan, K.-S. Hong, and A. Basit, "Event-triggered leaderless robust consensus control of nonlinear multi-agents under disturbances," in *Proc. 13th Asian Control Conf. (ASCC)*, May 2022, pp. 1736–1741.

[16] A. Basit, M. Tufail, K.-S. Hong, M. Rehan, and I. Ahmed, "Event-triggered distributed exponential h8 observers design for discrete-time nonlinear systems over wireless sensor networks," in *Proc. 13th Asian Control Conf. (ASCC)*, May 2022, pp. 1730–1735.

[17] W. Xu, S. Qu, and C. Zhang, "Fast terminal sliding mode current control with adaptive extended state disturbance observer for PMSM system," *IEEE J. Emerg. Sel. Topics Power Electron.*, vol. 11, no. 1, pp. 418–431, Feb. 2023.
[18] Z. Zhang, X. Liu, J. Yu, and H. Yu, "Time-varying disturbance observer based improved sliding mode single-loop control of PMSM drives with a hybrid reaching law," *IEEE Trans. Energy Convers.*, early access, May 18, 2023, doi: 10.1109/TEC.2023.3277628.
[19] T. H. Nguyen, T. T. Nguyen, V. Q. Nguyen, K. M. Le, H. N. Tran, and J. W. Jeon, "An adaptive sliding-mode controller with a modified reduced-order proportional integral observer for speed regulation of a permanent magnet synchronous motor," *IEEE Trans. Ind. Electron.*, vol. 69, no. 7, pp. 7181–7191, Jul. 2022.
[20] W. Liu, S. Chen, and H. Huang, "Adaptive nonsingular fast terminal sliding mode control for permanent magnet synchronous motor based on disturbance observer," *IEEE Access*, vol. 7, pp. 153791–153798, 2019.
[21] A. K. Junejo, W. Xu, C. Mu, M. M. Ismail, and Y. Liu, "Adaptive speed control of PMSM drive system based a new sliding-mode reaching law," *IEEE Trans. Power Electron.*, vol. 35, no. 11, pp. 12110–12121, Nov. 2020.
[22] T. Li, X. Liu, and H. Yu, "Backstepping nonsingular terminal sliding mode control for PMSM with finite-time disturbance observer," *IEEE Access*, vol. 9, pp. 135496–135507, 2021.
[23] E. Lu, W. Li, X. Yang, and Y. Liu, "Anti-disturbance speed control of low-speed high-torque PMSM based on second-order non-singular terminal sliding mode load observer," *ISA Trans.*, vol. 88, pp. 142–152, May 2019.
[24] L. Yuan, Y. Jiang, L. Xiong, and P. Wang, "Sliding mode control approach with integrated disturbance observer for PMSM speed system," *CES Trans. Electr. Mach. Syst.*, vol. 7, no. 1, pp. 118–127, Mar. 2023.
[25] X. Zhang, K. Zhao, L. Sun, and Q. An, "Sliding mode control of permanent magnet synchronous motor based on a novel exponential reaching law," *Proc. CSEE*, vol. 31, no. 15, pp. 47–52, 2011.
[26] X. Zhang, L. Sun, K. Zhao, and L. Sun, "Nonlinear speed control for PMSM system using sliding-mode control and disturbance compensation techniques," *IEEE Trans. Power Electron.*, vol. 28, no. 3, pp. 1358–1365, Mar. 2013.
[27] A. Apte, V. A. Joshi, H. Mehta, and R. Walambe, "Disturbance-observer-based sensorless control of PMSM using integral state feedback controller," *IEEE Trans. Power Electron.*, vol. 35, no. 6, pp. 6082–6090, Jun. 2020.
[28] L. Zhang, J. Bai, and J. Wu, "SPMSM sliding mode control based on the new super twisting algorithm," *Complexity*, vol. 2021, pp. 1–9, Jul. 2021.
[29] Y.-R. Li and C.-C. Peng, "Super-twisting sliding mode control law design for attitude tracking task of a spacecraft via reaction wheels," *Math. Problems Eng.*, vol. 2021, pp. 1–13, Mar. 2021.
[30] J. A. Moreno and M. Osorio, "A Lyapunov approach to second-order sliding mode controllers and observers," in *Proc. 47th IEEE Conf. Decis. Control*, Dec. 2008, pp. 2856–2861.
[31] A. Davila, J. A. Moreno, and L. Fridman, "Optimal Lyapunov function selection for reaching time estimation of super twisting algorithm," in *Proc. 48h IEEE Conf. Decis. Control (CDC) Held Jointly, 28th Chin. Control Conf.*, Dec. 2009, pp. 8405–8410.
[32] J. A. Moreno, "A linear framework for the robust stability analysis of a generalized super-twisting algorithm," in *Proc. 6th Int. Conf. Electr. Eng., Comput. Sci. Autom. Control (CCE)*, Jan. 2009, pp. 1–6.
[33] L. Derafa, A. Benallegue, and L. Fridman, "Super twisting control algorithm for the attitude tracking of a four rotors UAV," *J. Franklin Inst.*, vol. 349, no. 2, pp. 685–699, Mar. 2012.
[34] G. Duan and H. Yu, *LMIs in Control Systems: Analysis, Design and Applications*. Boca Raton, FL, USA: CRC Press, 2013.
[35] G. Duan and H. Yu, *LMIs in Control Systems: Analysis, Design and Applications*. Boca Raton, FL, USA: CRC Press, 2013.

MINGYUAN HU received the B.S. degree from the Department of Electronic and Electrical Engineering, Sungkyunkwan University (SKKU), Seoul, South Korea, in 2021, where he is currently pursuing the Ph.D. (M.S. and Ph.D. joint program) degree with the Department of Smart Fab. Technology. His current research interests include sliding mode control, quadrotor, and permanent-magnet synchronous motor.

HYEONGKI AHN received the B.S. degree in control and instrumentation engineering from Gyeongsang National University, in 2021. He is currently pursuing the M.S. degree with the Applied Optimization Laboratory, Sungkyunkwan University. His current research interests include system design, sliding mode control, machine learning method, and device free localization.

KWANHO YOU received the B.S. and M.S. degrees in electrical engineering from the Korea Advanced Institute of Science and Technology (KAIST), in 1993 and 1996, respectively, and the Ph.D. degree from the University of Minnesota, in 2000. He was a Faculty Member with Texas A&M University. In 2001, he joined the School of Information and Communication Engineering, Sungkyunkwan University. His research interests include nonlinear and optimal control, radio resource management in wireless communication, adaptive optimization methods in nonlinear process, and estimation theory.